

# Large flotation cells in copper processing: Experiences and considerations:

by D. Govender, D. Meadows, D. Lelinski and F. Traczyk

In recent years, economies of scale have continued to drive copper projects to larger throughputs to offset depleting lower grade resources. A decade ago there were only a small number of projects that stretched beyond 100 kt/d (110,000 stpd) throughput rates. Today, and moving forward, virtually all the major copper projects are sized beyond this, with throughput rates up to 250 kt/d (275,000 stpd) now under evaluation for a number of key projects in Chile and Peru. This paper explores the development from the 160 m<sup>3</sup> (5,650 cu ft) flotation cells, through to the 257 m<sup>3</sup> (9,076 cu ft) cells and to the current 660 m<sup>3</sup> (23,380 cu ft) machines. The contributions of specific copper concentrators to this growth phase are reviewed in this paper. The historical basis of flotation machine scale-up is also briefly discussed. Metallurgical results as well as layout, maintenance and operational aspects are highlighted.

### Introduction

It is often said that ore resource depletion, and the associated increase in mill throughput, perpetuates the development of process equipment. Lower ore quality and increased mineralogical complexity are projected to continue in the near term. But, that is a controllable risk. There is an abundance of the commodity (1 x 10<sup>14</sup> metric tons in the upper kilometer of the earth's crust), but the extraction of the ore is anticipated to only increase in difficulty and cost. Continual resource quality degradation suggests future potential for mechanical cell development. However, possible impediments do exist. It may be difficult to envisage an outcome where resource quality degrades as expected but copper metal production is not offset by increasing throughput. However, the following near-term scenarios are plausible:

- Alternative flotation technology that reduces residence time dependency through reduced fluid dispersion or the separation of collision and attachment sub-process.
  - Deployment of ore pre-concentration technology to remove waste rock prior to processing.
  - Copper supply gap filled by the secondary scrap metal market.
- Substantial decrease in commodity demand through metal substitution or general weak economic demand.

Since the 1950s, mechanical flotation machines have increased vastly in size, but their principle of operation remains essentially unchanged. Therefore, technologies that produce a higher mineral recovery per unit volume are possible flowsheet substitutions for existing technology. Feasible mineral pre-sorting/classification technology may be a few years away from successful commercial deployment. While it is anticipated that the secondary market will contribute a growing proportion to overall copper consumption over the long term, short-term trends still favor existing and new mined supply. Overall, the greatest short term risk to future large cell development appears to be macroeconomic in nature. Copper consumption may be viewed as a proxy for economic activity. Global copper production, expected to increase to 17 Mt (18.7 million st) in 2013, suggests that there still is significant demand for the metal.

During the 1990s, many marginal copper producers were shuttered as the metal price offered no significant premium. During this time, mechanical flotation machine development also stagnated, as the rate of increase of individual cell volume failed to match that of previous decades. In the past decade, as the copper price quadrupled, so has the individual cell volume of mechanical flotation machines. It is probably safe to say that large flotation machine development is fundamentally contingent upon a favorable underlying copper commodity price.

### Copper price drivers

Primary copper mine grades have dropped steadily over the last 60 years. This trend is likely to continue as the discovery and exploitation of relatively high-grade deposits is likely to be anomalous over the coming years. Newer technologies are likely to improve extraction efficiency, but overall, the cost of extraction is likely to increase. Copper prices also remain elevated by historical standards, and regression to the mean is probable. The copper price incentive to pursue new projects and expansions is bound to increase, although commodity price stability rather than absolute highs may offer greater investment confidence. Like most commodities, copper price trends are, on average, a response

**D. Govender, D. Meadows, D. Lelinski and F. Traczyk, are..... with FLSmidth, email Sean. Dariusz.Lelinski@flsmidth.com.**

**Table 1**

Copper mined average grade decline — selected operations.

Operation	Year 2000	Year 2011
Escondida	1.9	1.2
Collahuasi	1.6 <sup>a</sup>	1.1
Los Pelambres	1.0	0.8
Codelco	-	0.8
<sup>a</sup> refers to year 2003		

to market economics. Copper prices, though, are unique in their ability to gage the strength of the global economic engine. Copper demand may have been previously skewed toward western industrial activity and the telecommunications boom. However, in the past decade, the strength in copper prices has been driven by the rapid urbanization of India and China's populations. The housing, automobile and railway industries are significant contributors to copper demand. Additionally, global investors seeking riskier assets have, in general, shifted their emphasis toward commodities, initiating long-term support for all commodities since the beginning of the 21st century.

### Threats

The near-term consumption trend still favors copper demand over supply. Part of the supply gap is expected to be filled by new supply in the primary market. The recently commissioned Antofagasta Minerals Esperanza operation is an example of this. It is anticipated that a growing percentage of that gap will be filled by the secondary market comprising scrap metal. The dynamic supply-demand balance is affected by a multitude of factors. Labor unrest and mining tax reform have become commonplace as copper prices trade at a premium to marginal production costs. Industrial action at Freeport McMoran's Grasberg operation had a significant adverse impact on copper concentrate production. Infrastructure constraints also prevail. Electricity grid supply in Chile and Zambia require upgrading. Chilean miner Codelco recently reported rising energy costs as a significant contribution to overall cash costs. The shift to salt water flotation at the Esperanza operation, coupled with novel magnesium precipitation technology forecasts a shift away from existing water supply constraints. Central bank monetary policy also affects global economic growth. Recent bias should be avoided as historical consumption trends should not be regarded as indicative of future demand, especially as macroeconomic risks abound. Resource quality is also a potential risk. However, resource quality is generally predictable over the longer term, and offers some insight into predicting the supply side of the equation.

### The resource quality effect

Primary ore quality, having declined substantially over the last century, poses a controllable risk to copper market supply. The rate of decline of an ore-body is characteristic of its geology (Table 1), and is anticipatory. The deflation of resource quality has been concomitant with an increase in extraction costs. Sustainably

high copper commodity prices, though, are attractive to producers willing to exploit the mid-to-low grade ore bodies.

Ore quality does not necessarily refer to ore grades alone. Ore hardness and mineralogical complexity are additional sub-components that dictate flowsheet development and processing equipment size and type. These are important factors to consider because, generally, the copper price incentive to bring new copper capacity online is most sensitive to the minimum attractive rate of return on the investment. Taxes, royalties, capital and operating expenditure are the next important factors to consider.

### Mechanical flotation machine characterization (selected parameters)

**Large cell development benefits.** Since the initial commercialization of flotation technology more than a century ago, the increase in individual cell volume (Fig. 1) has been attributable to declining resource quality offset by increasing mill throughput (Weber et al., 2005). Benefits have also been partially derived by leveraging the frequency of flotation machine scale-up, and ensuring a quicker time to market for the newer, larger machines. The benefits of large flotation machines include:

- Lower maintenance costs.

**Figure 1**

Wemco flotation machine development timeline.

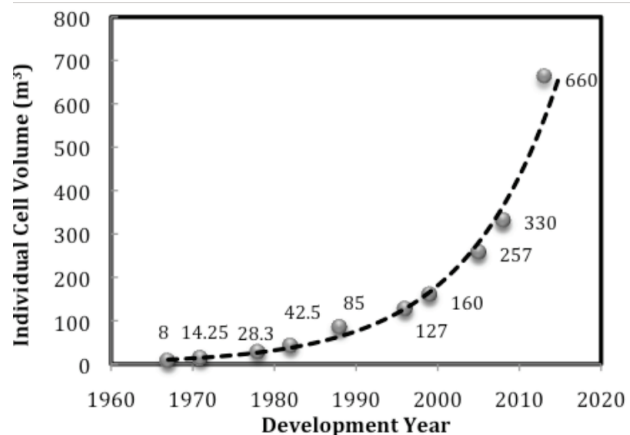
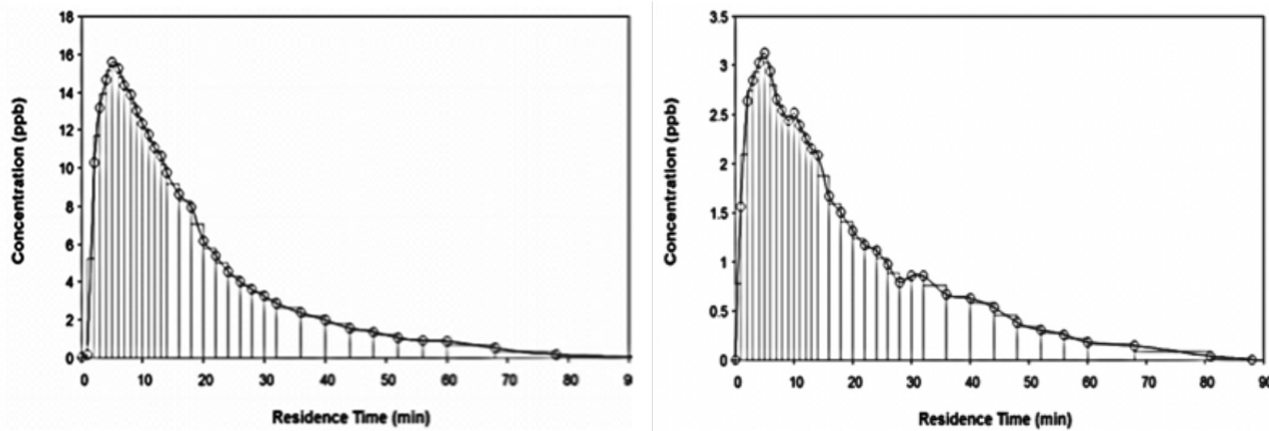


**Figure 2**

Residence time distribution profiles for the single-cell Wemco 300m<sup>3</sup> (left) and Dorr-Oliver 330m<sup>3</sup> (right).



- Lower installed costs.
- Reduced flotation area footprint.
- Shorter row lengths.
- Simplified sampling strategy.
- Ease of control.
- Reduced specific power consumption .

**Residence time distribution.** The residence time distribution is a useful diagnostic tool for evaluating:

- Pulp short-circuiting.
- Mechanical integrity.
- Loss of volume through sanding.
- Non-optimal gas hold-up.

Measurement techniques are aptly described by Nasset (1988), Weber et al. (2005) and Yianatos (2008, 2012a). Nasset (1988) proposes that a suitable tracer should be characterized by low cost, high relative detectability, convenience in preparation and analysis, and exhibit process non-interference. Lelinski et al. (2000) compare the residence time distribution profiles of 160 m<sup>3</sup> (5,650 cu ft) mechanical flotation machines in a comprehensive analysis. Liquid and solids residence times are compared by Weber et al. (2005) and Yianatos (2008, 2010). Weber et al. (2005) show solids residence times varying in the range of 92–95 percent of the liquid residence time. The liquid phase residence time distributions for the single-cell 300 m<sup>3</sup> (11,654 cu ft) Wemco and 330 m<sup>3</sup> (11,654 cu ft) Dorr-Oliver machines are shown in Fig. 2.

These profiles are indicative of reasonably good flow, and the absence of sharp, early peaks qualitatively eliminates liquid short-circuit phenomena (Nelson et al., 2002). The application of residence time distributions to circuit design is discussed later on.

### Bubble surface area flux ( $S_b$ )

Harbort and Schwarz (2010) detail available

instrumentation, and the application of techniques to large flotation machine characterization. The superficial gas rate and Sauter mean bubble diameter parameters contributing to the bubble surface area flux response are often measured during the characterization of large flotation machines (Table 4). Generally, the  $S_b$  data is then reported and merely compared to previously reported industrial-scale data. Yianatos et al. (2010) utilize the bubble surface area flux data to compare the collection zone rate constant ( $K\tau$ ) for the OK-160 and OK-300, concluding similar efficiencies between both machines.

The flotation rate constant ( $k$ ) should yield a positive linear dependence on the bubble surface area flux (Gorain, 1997; Jameson et al., 1977). Grönstrand et al. (2010) and Yanez et al. (2009) attempt to corroborate this linear dependence by fitting a linear regression trend to selective data points in the evaluation of the OK-300 machine. The data suggest no relationship between the independent and dependent variables of  $S_b$  and copper/molybdenum recovery, respectively. In fact, linear regression analysis through all data points would yield a negative correlation between copper recovery and bubble surface area flux. Yanez et al. (2009) suggests that at high bubble surface area flux “a new factor is at play.” It should be noted that Grönstrand et al. (2010) and Yanez et al. (2009) fail to decouple the collection zone and overall rate constants. The  $k$ - $S_b$  linear dependence is valid at higher mass pull conditions (Gorain, 1997), where the collection zone kinetic rate is the main effect. The OK-300 machine was operated at the head of a rougher row, where a deeper operating froth depth would have been selected. At deeper froth depths, the froth recovery component dominates over collection zone kinetics, rendering the  $k$ - $S_b$  relationship invalid. Yanez et al. (2009) also present the residence time and bubble surface area interaction. These results suggest that froth carrying capacity has constrained overall copper and molybdenum kinetics.

**Table 2**  
Sampling of large mechanical flotation machine bubble surface area flux measurements.

Machine Type: Volume (m <sup>3</sup> )	S <sub>b</sub> -value (m <sup>2</sup> /s/m <sup>2</sup> )	Source
OK-300: 300	44.5	Yianatos et al. (2010)
OK-160: 160	41.7	Yianatos et al. (2010)
OK-160: 160	24 – 42	Yianatos et al. (2012a)
OK-300: 300	19.8 – 57.7	Yanez et al. (2009)
OK-200: 200	27.0 – 40.5	Yianatos et al. (2012b)
Dorr-Oliver: 330	41.5 – 71.6	Govender et al.

**Metallurgical characterization - introduction**

Degner (1995) remarked that the metallurgical evaluation of single-cell prototypes should not be the main objective. Single machines are subject to pulp short-circuiting and mixing theory suggests that metallurgical performance would be inferior to smaller, serially arranged machines of equal volume. The reduction of froth carrying capacity is also likely to preferentially result in the loss of the coarse fraction. But a large flotation machine that fails to replicate the metallurgical performance of smaller machines in a side-by-side trial would probably be viewed as a failure. Lelinski et al. (2012) detail the successful metallurgical evaluation of a single large machine operating against four smaller units of similar total volume. Weber et al. (2005) compare a large machine operating in parallel to smaller units at the head of the rougher flotation. The one- vs. two-cell scenario is adopted in this instance. The tails streams from these large machine prototypes are re-routed back to the head of the rougher row, thereby providing additional residence time while in operation. This arrangement also mitigates the risk associated with prototype downtime. These large machines are often tested to evaluate their metallurgical performance and mechanical integrity in lieu of concentrator expansion and machine incorporation into the flowsheet incorporation. There may be additional symbiotic relationships for machine supplier and end-user when testing large flotation machines. (Dunn et al. 2009) describe the use of the Wemco 300 m<sup>3</sup> (11,654 cu ft) SuperCell in a cleaner duty debottlenecking exercise.

**Design considerations**

**Layout considerations.** Arbiter (2000) was a proponent of the 12-cell minimum rougher row, stating a preference for 14 serially arranged machines to eliminate pulp short-circuiting. Moreover, he indicated that this constraint would be prohibitive to large mechanical cell development. The cells-in-series requirement is predicated upon the attribute of perfect mixing in flotation machines. In adopting classical mixing theory, impetus is given to unanimity on the cell quantity selection criterion. However, Nasset (1988) reports a sampling of recommended minimum cell row lengths (in terms of the cell quantity), where the suggested number of serially-arranged machines ranges from four to 18.

There is difficulty in accepting standardized row lengths (Table 3). Mineralogy, liberation characteristics, feed grade, size distribution, pulp chemistry and flotation mechanism type

often differ for similar applications. The effect of short-circuiting on metallurgical performance of smaller flotation machines was observed during the evaluation of the 28.3 m<sup>3</sup> (1,000 cu ft) Wemco machine. Actual pulp residence time approached half of the machine’s theoretical value. Degner (1995) cautioned against the use of less than six cells in a row. Although not quantified, the effect of connection boxes on short-circuiting is mentioned by Churchill and Degner (1982). They suggested a maximum cell-bank length limitation of 12.2 m (40 ft) between connection boxes to minimize hydraulic gradient variations between connection boxes. This obviously constrained the number of internally-baffled rectangular machines that could be installed per bank as machine size increased. Currently, large cylindrical flotation machines are generally arranged as single cells

**Table 3**  
Sampling of row lengths for large mechanical flotation machines operating in bulk copper rougher-scavenger duty.

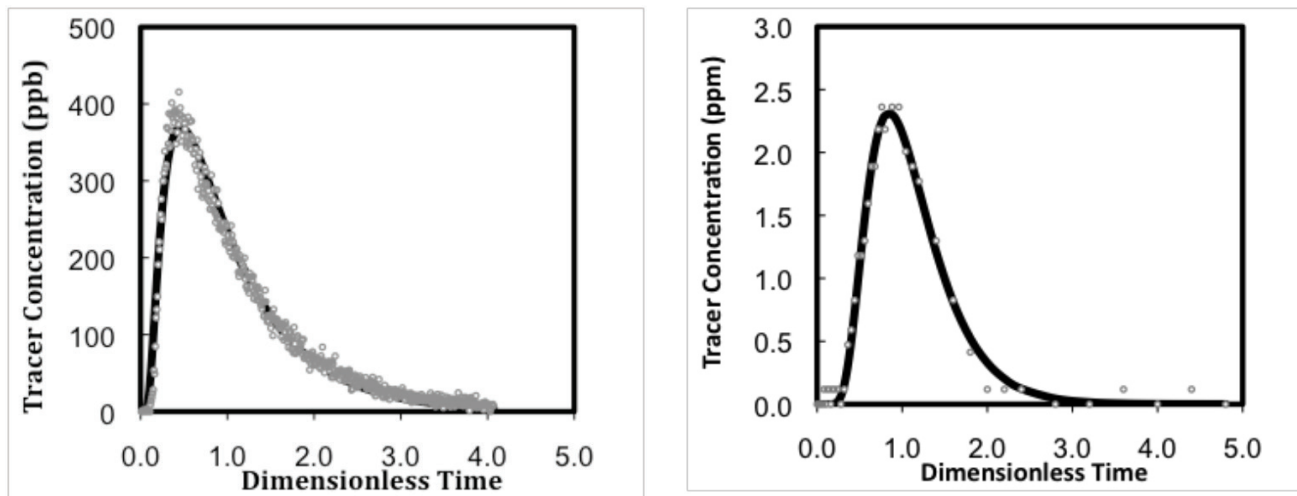
Machine type: Volume (m <sup>3</sup> )	Cells-in-series	Concentrator
Wemco: 257	9	Mineral Park
Wemco: 257	5	Los Pelambres
Wemco: 300	6	Collahuasi
Wemco: 300	7	Esperanza
Wemco: 160	7	Lumwana
Wemco: 160	9	Escondida (Yianatos et al. 2006)
OK-160: 200	9 <sup>b</sup>	Carmen de Andacollo (Yianatos et al. 2012b)
OK-160: 160	8	Codelco Norte Division (Yianatos et al. 2010)
OK-160: 160	9	Collahuasi (Yianatos et al. 2012a)

<sup>b</sup> Includes a single pre-rougher machine.

# Base Metals

**Figure 3**

Residence time distribution for the Wemco 257 m<sup>3</sup> single cell (left) and five cell row (right).



per bank, although the installation of two 160 m<sup>3</sup> (5,650 cu ft) machines per bank is still considered acceptable. In the latter instance, operational flexibility is sacrificed for the capital cost saving. In large machines, the inter-tank connection box design has also been simplified. This has resulted in reduced total row length (distance) and a lower secondary contribution of connection boxes to the short-circuiting phenomenon.

The measurement and analysis of residence time distributions should have primary focus on the estimation of short-circuiting and dead volume contributions applicable to the vessel of interest. The effect of cell mixing on metallurgical performance may be quantified by the fluid dispersive intensity within a flotation machine. Figure 3 compares the single-cell and five-cell

liquid tracer curves. The measurements were produced at two different concentrators although unit-cell theoretical mean residence times were comparable. In Figure 4, the theoretical collection zone recovery is bound by the plug flow and single-cell perfectly-mixed flow recovery profiles.

The fitted tracer data are used to predict and compare the fluid dispersion of the single- and five-cell options (Fig. 4). The theoretical collection zone recovery profiles for these two conditions are compared. Figure 4 suggests that the single-cell fluid dispersion behavior of large Wemco flotation machines is not adequately described by the perfect-mixing model. Similarly, the fluid dispersion of the five-cell row is indicative of the six cells-in-series perfect mixing model. This has consequences for scale-up from smaller machines, as the perfect mixer model would underpredict the performance of larger machines, especially for short-row lengths.

A basic comparison was performed to show the general effect of mechanical flotation machine size on the following responses:

- Flotation machine capital equipment cost.
- Absorbed power.
- Floor space requirements.
- Platform elevation requirements.

These responses are evaluated as a function of the following parameters:

- Individual cell volume — 160; 250; 300 m<sup>3</sup> (5,650; 8,282; 10,594 cu ft).
- Dry solids throughput — 150; 200; 250 ktpd (165,000; 220,000; 275,000 stpd).
- Feed solids concentration (35 percent w/w).
- Solids specific gravity (2.7).
- Slurry residence time (15 min.).
- Equipment utilization (100 percent).

**Figure 4**

First-order theoretical recovery related to vessel fluid dispersion and degree of reaction completion.

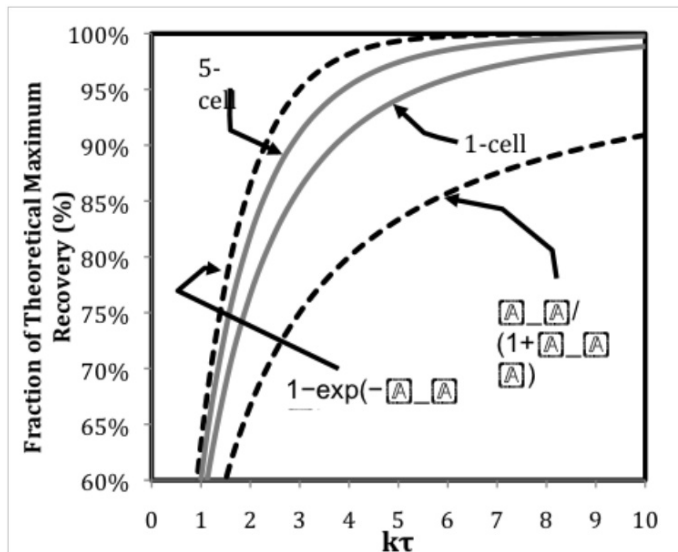
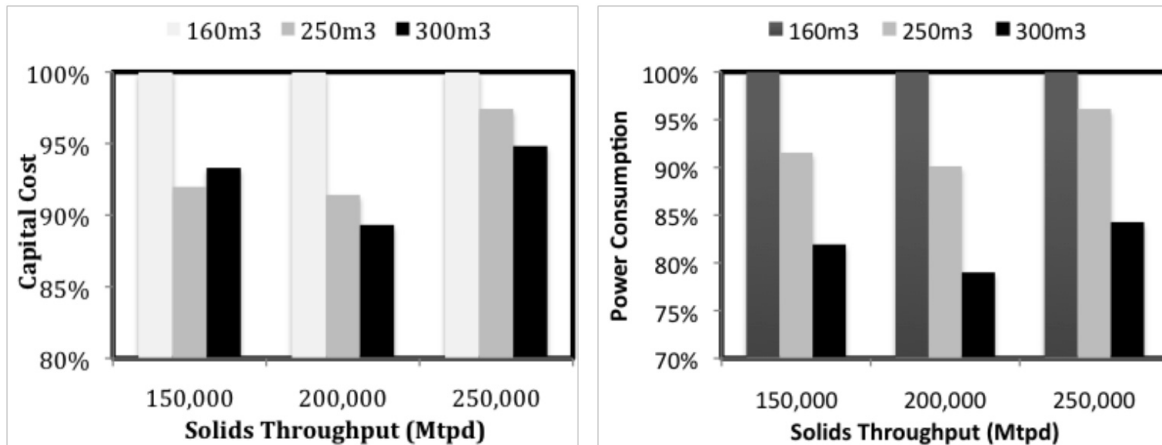


**Figure 5**

Comparison of equipment capital cost (left) and power consumption (right).



Hypothetical flotation rows were arranged with the following constraints:

- The number of machines per row was constrained to the range of 6–9 cells.
- The 160 m<sup>3</sup> (5,650 cu ft) machine was limited to a maximum of two cells per bank.
- The 250 m<sup>3</sup> and 300 m<sup>3</sup> (8,828 cu ft and 10,594 cu ft) machines were limited to a maximum of one cell per bank.

No maximum row length (in terms of distance), floor area or elevation restrictions were applied.

Figure 5 illustrates the equipment capital cost and power consumption comparison as a function of throughput and individual cell volume. Potential savings are displayed as a function of the 160 m<sup>3</sup> (5,650 cu ft) baseline case. Power values represent absorbed power intensity (kW/m<sup>3</sup>) under a water-only condition. Relative power consumption suggests significant benefits for the 250 m<sup>3</sup> and 300 m<sup>3</sup> (8,828 and 10,594 cu ft) machines. The 150 kt/d and 200 kt/d (165,000 and 220,000 stpd) options approximate the capital equipment savings provided by Weber et al. (2005) for a 100 kt/d (110,000 stpd) option. There is reduced capital cost benefit for the 250 kt/d (275,000 stpd) scenario, suggesting a potential tipping point in favor of a larger available cell size. In general, the selection of large flotation machines offers the greatest capital cost benefit with regard to machine installation.

The floor space requirements are presented in the form of a linear interaction model in Figure 6. The floor area requirement is dependent on the selection of the individual machine volume and solids dry throughput variables. The floor area is then estimated from the row length, row quantity and row width. Access and auxiliary equipment area requirements between parallel rows are not accounted for. The constant slopes of the models indicate a constant area requirement per unit

throughput for the range of scenarios tested. Area requirements for the 250 and 300 m<sup>3</sup> (8,828 and 10,594 cu ft) machines range from 75–80 percent of the baseline case.

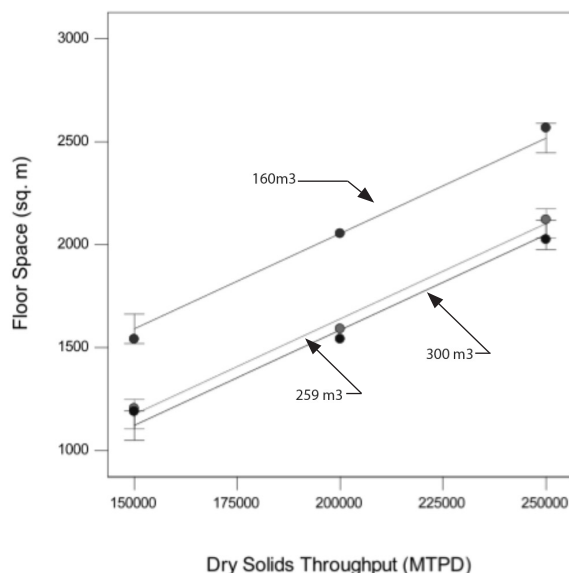
Pulp level control is realized through elevation changes in a gravity flow system. The interstage step heights are driven by the following variables:

- Dart valve plug and grommet sizes
- Dart valve quantity
- Actuator design and availability
- Flowrate (Velocity) through connection boxes

Generally, the standard interstage elevation drop corresponding to the individual cell volume is initially selected (Fig. 7), and the valve size

**Figure 6**

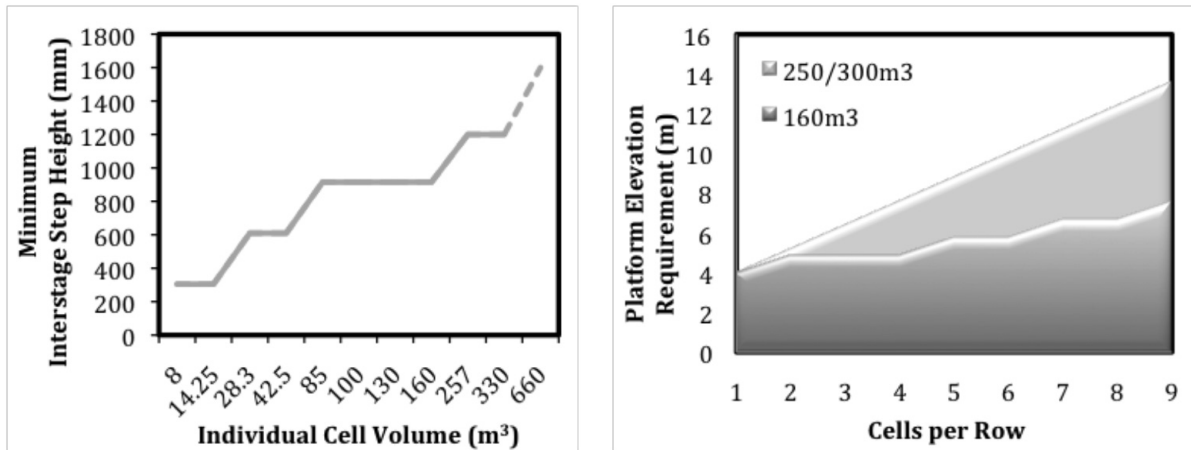
Effect of throughput and machine selection on floor space requirements.



# Base Metals

**Figure 7**

Effect of individual machine volume on recommended interstage elevation change (left), and flotation machine platform elevation requirements as a function of cell quantity and volume (right).



calculated thereafter. On larger flotation machines, the recommended valve quantity is two valves per level control system. Figure 7 indicates the effect of individual cell volume on minimum interstage step height, and the cumulative effect of serially arranged machines on the cell platform elevation requirement. An arbitrary initial height 4 m (13 ft) is chosen for sub-cell access, and discharge sump installation. An optional practice involves using a raised discharge outlet to minimize this initial height, thereby reducing the overall height requirement. As the row elevation increases, so too does the final clearance requirement for mechanism removal.

The operating and mechanism removal clearance heights are shown in Figure 8. These dimensions are relative to the tank bottom. The operating heights are similar due to the drive mechanism transition from v-belt to gearbox option for machine volumes exceeding 160 m³ (5,650 cu ft). Also, geometric scale-up results in a

greater effect of tank diameter on tank volume.

It is common to support the flat-bottomed tank design of large flotation machines on a concrete base. The selection of elevated or ground-supported bases is related to topographical considerations, as flotation circuits are typically gravity-fed. The addition of steel grillage (Fig. 9a) augments installation costs, but does allow for inspection of the tank bottom.

### Circuit design

Large bulk copper flotation circuits are typically designed around open-circuit roughing and closed-circuit cleaning principles. In general, flotation circuit designers utilize larger machines in rougher-scavenger duty, complemented by smaller machines in the cleaner and cleaner-scavenger duties. This is typical in most flotation applications, as the slurry volumetric flow to the cleaning circuit is a fraction of the total feed. Additionally, faster rougher concentrate flotation kinetics imply lower

**Figure 8**

Machine operating height and mechanism removal clearance height (left), and cumulative mechanism clearance height requirement as a function of cell position and individual cell volume (right).

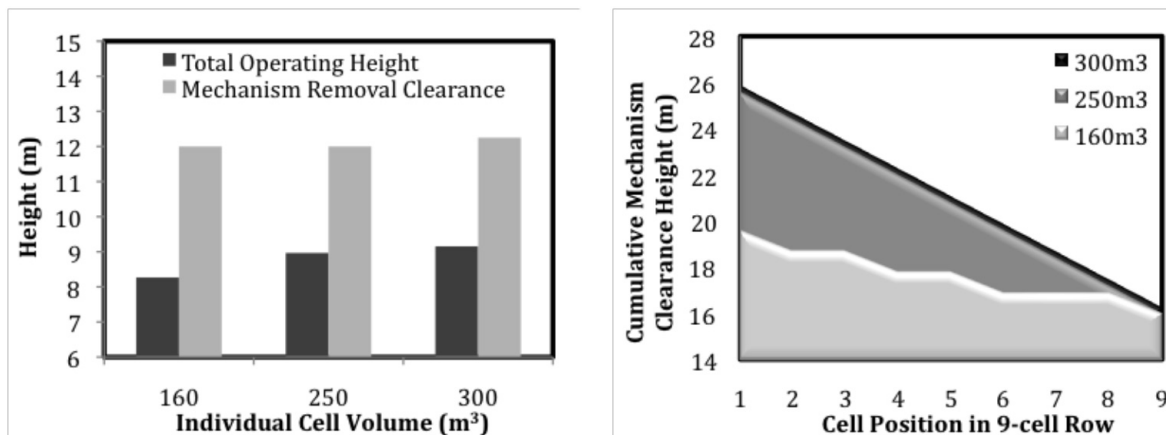


## Figure 9

Variations in platform design for machine sizes in the range of 257 – 300 m<sup>3</sup> (Mineral Park Phase II – left; Esperanza – middle; Penasquito – right).



residence time and cells-in-series requirements for the cleaning circuit. The recent trend on large copper concentrators shows a shift towards using the same individual cell volumes on both roughing and cleaning duties. Commonality of spares is an obvious benefit, but this also represents a favorable change in perception toward the acceptance of larger machines in the shorter row lengths of cleaning circuits.

Large circuits are also incorporating the Mixed-Row and Mixed-Circuit technologies. The former refers to the use of both forced-air and induced-air mechanical machines in a single flotation row. The latter refers to the use of forced-air and induced-air mechanical machines in different duties. These configurations offer the end-user the option to customize their large flotation circuits according to their specific grade and recovery requirements. Hybrid Energy Flotation has also been successfully incorporated into flotation circuits. Flotation rows designed according to this concept take advantage of variations in the energy input in the flotation row to target specific particle size classes. Overall energy consumption is not increased as energy consumption is increased to optimize the bubble-particle collision sub-process, but reduced to improve coarse fraction recovery.

### Conclusions

Mechanical flotation machine development has been and will continue to be driven by resource quality degradation and the associated throughput compensation. The near term primary market for large flotation machines remains in the copper concentrators of Chile and Peru. The contribution of large concentrators in emerging copper producers like Kazakhstan and Mongolia is also expected to increase. Revenue and costs are intuitively obvious factors dictating the rate of return on capital for new mine supply or expansion projects. As extraction costs increase, operational viability becomes increasingly dependent on the metal price trading at a significant margin. Therefore, the copper commodity price is a key

driver. The use of large mechanical machines is often easily justifiable due to reduced equipment capital, installation and operating costs, relative to previous generation machines.

### Future design considerations

Mechanical flotation machines are designed to be multifunctional. Solids suspension, air and fluid dispersion are linked to the sub-processes of bubble-particle collision, attachment and detachment. Moreover, optimal froth transport characteristics are required to maximize valuable mineral recovery across all size classes in a single machine. This leads to cumulative inefficiencies in a single machine as these series of actions need to be balanced. Machines that separate the collection zone and froth phase recovery sub-processes are likely to gain favor. In existing machines that incorporate both sub-processes, greater focus is required to improve froth transport characteristics. The magnitude of the froth recovery effect will obviously vary as a function of application and duty, but initial pre-concentration of slurries can use the existing design of mechanical machines. For decades, the industry has been searching for a substitute to the large mechanical flotation machine. If the metallurgical efficiency plateau is to be surpassed, the alternative solution lies in merging the benefits of large mechanical flotation machines with the efficiency improvements of newer technology. (References available from the authors.) ■

### Acknowledgements

The authors thank Bartosz Dabrowski of FLSmidth Salt Lake City, Inc. for assistance with characterization measurements and data analysis. Bob Rodgers and Ken Leader for permission to publish the Mineral Park data. Dave Rollins and Brad Gerke of FLSmidth Salt Lake City, Inc. for assistance with circuit configurations and cost estimation and Gerald Luttrell and his team at Virginia Tech for assistance with characterization measurements.